

LEVEL 1:
BE UNDERSTANDABLE



THESE ARE JUDGES.
(OR MAYBE YOUR MOM.)

LEVEL 1:
BE UNDERSTANDABLE



THESE ARE JUDGES.
(OR MAYBE YOUR MOM.)

They can't love you if
they don't know what
you're talking about.



LEVEL 1:
BE UNDERSTANDABLE



1. DITCH THE JARGON.
2. REDUCE THE CONTENT.
3. ORGANIZE WHAT'S LEFT.

LEVEL 1:
BE UNDERSTANDABLE



1. DITCH THE
JARGON.

Centrality Measures of Graphs utilizing Continuous Walks in Hilbert Space

Jarod Benowitz¹, David Peak¹, PhD

¹Utah State University, Physics Department, UT 84321, Email: JarodPBenowitz@Gmail.com



ABSTRACT

Centrality is most commonly thought of as a measure in which we assign a ranking of the vertices from most important to least important. The importance of a vertex is relative to the underlying process being carried out on the network. This is why there is a diverse amount of centrality measures addressing many such processes. We propose a measure that assigns a ranking in which interference is a property of the underlying process being carried out on the network.

INTRODUCTION

Networks are perhaps one of the most ubiquitous structures in nature. They arise for example in cellular biology connecting genes and proteins, in neuroscience connecting neurological regions of the brain, in sociology connecting the interactions of people, and recently in quantum computing. The analysis of the underlying topology of these discrete structures has thus gained widespread attention. Likewise, there has been a significant focus on designing measures to assess certain topological features of a network by assigning quantitative values to the nodes. These quantitative values have a subtle interpretation insofar as there are implicit assumptions of the underlying process being carried out on the network.

Borgatti has identified a typology of flow processes with specific trajectories that use trails, geodesics, paths, or walks. In this framework the flow has a specific type of transmission corresponding to some concrete application. Borgatti gives examples such as used goods, currency, infections, and gossip. Suppose we want to model a flow process in which the flow may interfere with itself. This interference may be the result of collisions in the network where oppositely oriented flows may annihilate. How then can we model such a flow? Our proposition is to model continuous walks on the network insofar as interference becomes an emergent property.

Definition: Centrality is a measure in which the nodes of a network are assigned a ranking with respect to an implicit assumption of the flow characteristics of the network. Below we give several examples of common centrality measures.

Degree Centrality: $\text{deg}(i) = \sum_{j=1}^N a_{ij} = (\mathbf{A}\mathbf{e})_i$

Katz Centrality: $\kappa(i) = \sum_{j=1}^N \sum_{k=0}^{\infty} \alpha^k (A^k)_{ij} = ((I - \alpha A)^{-1} - I)\mathbf{e}_i$

Closeness Centrality: $C(i) = \left[\sum_{j=1}^n d(i,j) \right]^{-1}$

THEORY

lemma 1.1: The power-law function $f(x) = \alpha^x$, $x \in \mathbf{R}$ of the adjacency matrix produces complex functions as the entries.

Proof: Let \mathbf{A} be the adjacency matrix of a simple nonempty graph. \mathbf{A} is a traceless symmetric matrix, $\text{Tr}[\mathbf{A}] = [\mathbf{A}, \mathbf{A}^T] = 0$. Since it is symmetric it is always diagonalizable, we then have $\mathbf{A} = \mathbf{P}\mathbf{D}\mathbf{P}^{-1}$ where \mathbf{P} are the eigenvectors collected as a matrix and \mathbf{D} is the diagonal matrix consisting of the eigenvalues of \mathbf{A} . We then have $\text{Tr}[\mathbf{A}] = \text{Tr}[\mathbf{P}\mathbf{D}\mathbf{P}^{-1}] = \text{Tr}[\mathbf{D}(\mathbf{P}\mathbf{P}^{-1})] = \text{Tr}[\mathbf{D}] = \sum_i \lambda_i = 0$. Since the graph is nonempty and the sum of the eigenvalues is zero we are therefore guaranteed to have at least one negative eigenvalue. The function of a matrix can be expressed as $f(\mathbf{A}) = \mathbf{P}f(\mathbf{D})\mathbf{P}^{-1}$, where the spectral decomposition is,

THEORY

$$\mathbf{A}^x = \mathbf{P}\mathbf{D}^x\mathbf{P}^{-1} = \sum_{i \in \Lambda^+ \setminus \{0\}} \lambda_i^x u_{ij} u_{jk} + \sum_{i \in \Lambda^-} \lambda_i^x u_{ij} u_{jk}$$

and where $(-\lambda)^x = \lambda^x e^{i\pi x}$. We then can express every entry of \mathbf{A}^x as,

$$\varphi_{jk}(\lambda, x) = \sum_{i \in \Lambda^+ \setminus \{0\}} \lambda_i^x u_{ik} + e^{i\pi x} \sum_{i \in \Lambda^-} \lambda_i^x u_{ik}$$

where $\Lambda^+ \setminus \{0\}$ is the multiset of all positive eigenvalues not including zero and Λ^- is the multiset of all negative eigenvalues. Since we are guaranteed at least one negative eigenvalue $\varphi_{jk}(\lambda, x)$ is complex always ■

Theorem 1.1: The Pairwise Walk Function (PWF), φ_{jk} , is an element of Hilbert Space.

Proof:

$$\int_0^1 \varphi_{jk}^* \varphi_{jk} dx = \sum_{i \in \Lambda^+} u_{ik}^2 \frac{\lambda_i^{2x-1}}{2 \ln(\lambda_i)} + 2 \sum_{i \in \Lambda^-} u_{ik}^2 \frac{(\lambda_i)^{2x-1} - 1}{\ln(\lambda_i^2)} + 2 \sum_{i \in \Lambda^+ \setminus \{0\}} u_{ij} \frac{\ln(\lambda_i \lambda_j) - \text{Re}(\lambda_i \lambda_j)^2 (\cos(\pi x) \ln(\lambda_i \lambda_j) + \pi \sin(\pi x))}{\pi^2 + (\ln(\lambda_i \lambda_j))^2}$$

On the right-hand side of the integral we have two indeterminates of the form $\frac{0}{0}$ when $\lambda_{i_n} \rightarrow 1$ and when $\lambda_{i_m} \rightarrow -1$. Upon a change of variable the limit is,

$$\lim_{x \rightarrow 2} \frac{x^2 - 1}{\ln(x)} = \lim_{x \rightarrow -2} \frac{x^2 - 1}{2 \ln(x)} = 1$$

The integral then converges over the interval and we have the desired result, $\varphi_{jk} \in \mathcal{H}_1$ ■ Below we plot the real and imaginary parts of several PWF's.

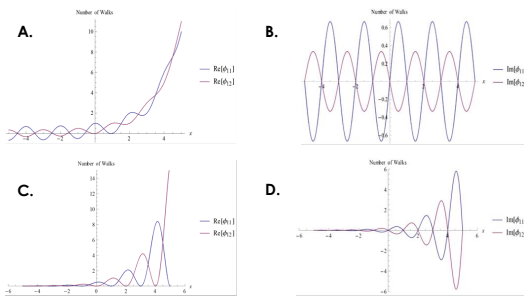


Figure 1. A & B) Real and imaginary parts of two PWFs for a complete graph on 3 vertices. C & B) Real and imaginary parts of two PWFs for a cycle graph on 4 vertices.

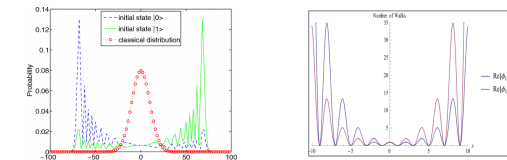


Figure 2. Numerical simulation of a Quantum Random Walk in 1D compared to the Real part of two PWFs for a path graph on 4 vertices.

RESULTS

Using the previous theorem we may now define a unique class of centrality measures that live in Hilbert Space. Moreover, we may generalize common centrality measures to account for the additional property of flow self-interference. Below we give *Degree-Interference* and *Closeness-Interference*, where ζ is the sum of the columns of the PWF matrix.

$$DI_j \equiv \|\zeta_j\| = \sqrt{\langle \zeta_j | \zeta_j \rangle} = \sqrt{\int_0^1 \zeta_j^* \zeta_j dx} = \sqrt{\int_0^1 \left(\sum_{k=1}^N \varphi_{jk} \right)^* \left(\sum_{k=1}^N \varphi_{jk} \right) dx}$$

$$CI_i \equiv \left[\sum_{j=1}^n d(\zeta_i, \zeta_j) \right]^{-1} = \left[\sum_{j=1}^n \|\zeta_i - \zeta_j\| \right]^{-1} = \left[\sum_{j=1}^n \sqrt{\langle \zeta_i - \zeta_j | \zeta_i - \zeta_j \rangle} \right]^{-1}$$

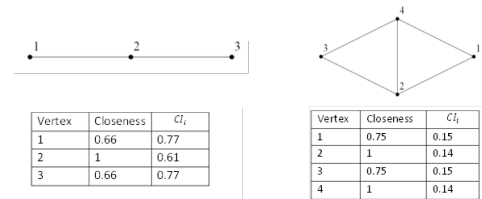


Figure 3. An inverse relationship between Closeness and Closeness-Interference. Closeness-Interference ranks the peripheral vertices closer than the core vertices. We may attribute this to destructive interference among the core vertices.

CONCLUSION

We've shown that when we allow continuous processes to occur on discrete structures interference becomes an emergent property. In this manner we view graphs as lower-dimensional discrete representations of Hilbert space. To the authors knowledge this is the first explicit relationship between combinatorics and Hilbert space. Using this to our advantage we've generalized several common centrality measures to account for flow self-interference. Furthermore, these measures may be used for the development of new and novel quantum algorithms. Likewise, we saw an interesting relationship between numerical simulations of quantum random walks in 1D with the PWF for the path graph. Keeping the Distance Minimizer theorem in mind, which states that for all vectors in Hilbert space there exists a unique vector in a closed subspace of Hilbert space, which minimizes their distance, we may utilize PWFs as approximations to quantum random walks. Finally, an intriguing prospect is whether or not we can construct linear hermitian operators corresponding to graph parameters just as we have linear hermitian operators that correspond to physical observables in quantum mechanics.

ACKNOWLEDGEMENTS

I thank Dr. David Brown for his constructive criticism and referee report of the paper. I also thank the Fall 2014 Graph Theory class for their constructive criticism.

REFERENCES

[1] C. M. Chandrashekar, R. Srikanth, and Subhashish Banerjee, Symmetries and Noise in Quantum Walk. Phys. Rev. A 76, 022316, 16 August 2007.
 [2] S. P. Borgatti and M. G. Everett, A graph-theoretic perspective on centrality, Social Networks, 28 (2006), pp. 466-484.

Centrality Measures of Graphs utilizing Continuous Walks in Hilbert Space

Jarod Benowitz¹, David Peak¹, PhD

¹Utah State University, Physics Department, UT 84321, Email: JarodPBenowitz@Gmail.com



ABSTRACT

Centrality is most commonly thought of as a measure in which we assign a ranking of the vertices from most important to least important. The importance of a vertex is relative to the underlying process being carried out on the network. This is why there is a diverse amount of centrality measures addressing many such processes. We propose a measure that assigns a ranking in which interference is a property of the underlying process being carried out on the network.

INTRODUCTION

Networks are perhaps one of the most ubiquitous structures in nature. They arise for example in cellular biology connecting genes and proteins, in neuroscience connecting neurological regions of the brain, in sociology connecting the interactions of people, and recently in quantum computing. The analysis of the underlying topology of these discrete structures has thus gained widespread attention. Likewise, there has been a significant focus on designing measures to assess certain topological features of a network by assigning quantitative values to the nodes. These quantitative values have a subtle interpretation insofar as there are implicit assumptions of the underlying process being carried out on the network.

Borgatti has identified a typology of flow processes with specific trajectories that use trails, geodesics, paths, or walks. In this framework the flow has a specific type of transmission corresponding to some concrete application. Borgatti gives examples such as used goods, currency, infections, and gossip. Suppose we want to model a flow process in which the flow may interfere with itself. This interference may be the result of collisions in the network where oppositely oriented flows may annihilate. How then can we model such a flow? Our proposition is to model continuous walks on the network insofar as interference becomes an emergent property.

Definition: Centrality is a measure in which the nodes of a network are assigned a ranking with respect to an implicit assumption of the flow characteristics of the network. Below we give several examples of common centrality measures.

Degree Centrality: $\text{deg}(i) = \sum_{j=1}^N a_{ij} = (Ae)_i$

Katz Centrality: $k(i) = \sum_{j=1}^N \sum_{k=0}^{\infty} a^k (A^k)_{ij} = ((I - \alpha A)^{-1} - I)e_i$

Closeness Centrality: $C(i) = \left[\sum_{j=1}^n d(i,j) \right]^{-1}$

THEORY

lemma 1.1: The power-law function $f(a) = a^x$, $x \in R$ of the adjacency matrix produces complex functions as the entries.

Proof: Let A be the adjacency matrix of a simple nonempty graph. A is a traceless symmetric matrix, $\text{Tr}[A] = [A, A^T] = 0$. Since it is symmetric it is always diagonalizable, we then have $A = PDP^{-1}$ where P are the eigenvectors collected as a matrix and D is the diagonal matrix consisting of the eigenvalues of A . We then have $\text{Tr}[A] = \text{Tr}[PDP^{-1}] = \text{Tr}[D(P P^{-1})] = \text{Tr}[D] = \sum_i \lambda_i = 0$. Since the graph is nonempty and the sum of the eigenvalues is zero we are therefore guaranteed to have at least one negative eigenvalue. The function of a matrix can be expressed as $f(A) = P f(D) P^{-1}$, where the spectral decomposition is,

THEORY

$$A^x = P D^x P^{-1} = \sum_i \lambda_i^x u_i u_i^T = \sum_i \lambda_i^x u_{ik}$$

and where $(-\lambda)^x = \lambda^x e^{i\pi x}$. We then can express every entry of A^x as,

$$\varphi_{jk}(\lambda, x) = \sum_{i \in \Lambda^+ \setminus \{0\}} \lambda_i^x u_{ik} + e^{i\pi x} \sum_{i \in \Lambda^-} \lambda_i^x u_{ik}$$

where $\Lambda^+ \setminus \{0\}$ is the multiset of all positive eigenvalues not including zero and Λ^- is the multiset of all negative eigenvalues. Since we are guaranteed at least one negative eigenvalue $\varphi_{jk}(\lambda, x)$ is complex always ■

Theorem 1.1: The Pairwise Walk Function (PWF), φ_{jk} , is an element of Hilbert Space.

Proof:

$$\int_0^L \varphi_{jk}^* \varphi_{jk} dx = \sum_{i \in \Lambda^+} \frac{u_{ik}^2 \lambda_i^{2x-1}}{2 \ln(\lambda_i)} + 2 \sum_{i \in \Lambda^+} \sum_{m \in \Lambda^+} \frac{(u_{ik} u_{im})^2 - 1}{\ln(\lambda_i \lambda_m)} + 2 \sum_{i \in \Lambda^+} \sum_{m \in \Lambda^-} \frac{\ln(\lambda_i \lambda_m) - (\lambda_i \lambda_m)^2 (\cos(\pi L) \ln(\lambda_i \lambda_m) + \pi \sin(\pi L))}{\pi^2 + (\ln(\lambda_i \lambda_m))^2}$$

On the right-hand side of the integral we have two indeterminates of the form $\frac{0}{0}$ when $\lambda_m \rightarrow 1$ and when $\lambda_n \lambda_m \rightarrow 1$. Upon a change of variable the limit is,

$$\lim_{x \rightarrow 1} \frac{x^L - 1}{\ln(x)} = \lim_{x \rightarrow 1} \frac{x^{2L} - 1}{2 \ln(x)} = L$$

The integral then converges over the interval and we have the desired result, $\varphi_{jk} \in \mathcal{H}_1$ ■ Below we plot the real and imaginary parts of several PWFs.

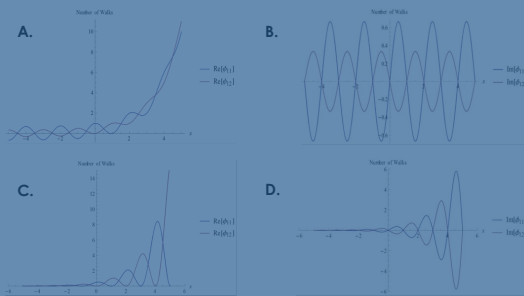


Figure 1. A & B) Real and Imaginary parts of two PWFs for a complete graph on 3 vertices. C & B) Real and Imaginary parts of two PWFs for a cycle graph on 4 vertices.

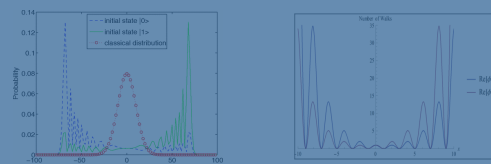


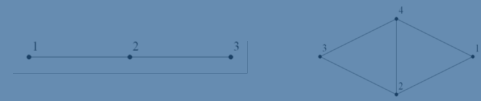
Figure 2. Numerical simulation of a Quantum Random Walk in 1D compared to the Real part of two PWFs for a path graph on 4 vertices.

RESULTS

Using the previous theorem we may now define a unique class of centrality measures that live in Hilbert Space. Moreover, we may generalize common centrality measures to account for the additional property of flow self-interference. Below we give Degree-Interference and Closeness-Interference, where ζ is the sum of the columns of the PWF matrix.

$$DI_j \equiv \|\zeta_j\| = \sqrt{\langle \zeta_j | \zeta_j \rangle} = \sqrt{\int_0^1 \zeta_j^* \zeta_j dx} = \sqrt{\int_0^1 \left(\sum_{k=1}^N \varphi_{jk} \right)^* \left(\sum_{k=1}^N \varphi_{jk} \right) dx}$$

$$CI_i \equiv \left[\sum_{j=1}^n d(\zeta_i, \zeta_j) \right]^{-1} = \left[\sum_{j=1}^n \|\zeta_i - \zeta_j\| \right]^{-1} = \left[\sum_{j=1}^n \sqrt{\langle \zeta_i - \zeta_j | \zeta_i - \zeta_j \rangle} \right]^{-1}$$



Vertex	Closeness	CI_i
1	0.66	0.77
2	1	0.61
3	0.66	0.77

Vertex	Closeness	CI_i
1	0.75	0.15
2	1	0.14
3	0.75	0.15
4	1	0.14

Figure 3. An inverse relationship between Closeness and Closeness-Interference. Closeness-Interference ranks the peripheral vertices closer than the core vertices. We may attribute this to destructive interference among the core vertices.

CONCLUSION

We've shown that when we allow continuous processes to occur on discrete structures interference becomes an emergent property. In this manner we may view graphs as lower-dimensional discrete representations of Hilbert space. To the authors knowledge this is the first explicit relationship between combinatorics and Hilbert space. Using this to our advantage we've generalized several common centrality measures to account for flow self-interference. Furthermore, these measures may be used for the development of new and novel quantum algorithms. Likewise, we saw an interesting relationship between numerical simulations of quantum random walks in 1D with the PWF for the path graph. Keeping the Distance Minimizer theorem in mind, which states that for all vectors in Hilbert space there exists a unique vector in a closed subspace of Hilbert space, which minimizes their distance, we may utilize PWFs as approximations to quantum random walks. Finally, an intriguing prospect is whether or not we can construct linear hermitian operators corresponding to graph parameters just as we have linear hermitian operators that correspond to physical observables in quantum mechanics.

ACKNOWLEDGEMENTS

I thank Dr. David Brown for his constructive criticism and referee report of the paper. I also thank the Fall 2014 Graph Theory class for their constructive criticism.

REFERENCES

[1] C. M. Chandrashekar, R. Srikanth, and Subhashish Banerjee, Symmetries and Noise in Quantum Walk. Phys. Rev. A 76, 022316, 16 August 2007.
 [2] S. P. Borgatti and M. G. Everett, A graph-theoretic perspective on centrality, Social Networks, 28 (2006), pp. 466-484.

Networks are perhaps one of the most ubiquitous structures in nature. They arise for example in cellular biology connecting genes and proteins, in neuroscience connecting neurological regions of the brain, in sociology connecting the interactions of people, and recently in quantum computing. The analysis of the underlying topology of these discrete structures has thus gained widespread attention. Likewise, there has been a significant focus on designing measures to assess certain topological features of a network by assigning quantitative values to the nodes. These quantitative values have a subtle interpretation insofar as there are implicit assumptions of the underlying process being carried out on the network.

Networks are perhaps one of the most ubiquitous structures in nature. They arise for example **in cellular biology connecting genes and proteins, in neuroscience connecting neurological regions of the brain, in sociology connecting the interactions of people, and recently in quantum computing.** The analysis of the underlying topology of these discrete structures has thus gained widespread attention. Likewise, there has been a significant focus on designing measures to assess certain topological features of a network by assigning quantitative values to the nodes. These quantitative values have a subtle interpretation insofar as there are implicit assumptions of the underlying process being carried out on the network.

Networks are perhaps one of the most ubiquitous structures in nature. They arise for example in cellular biology connecting genes and proteins, in neuroscience connecting neurological regions of the brain, in sociology connecting the interactions of people, and recently in quantum computing. The analysis of the underlying topology of these discrete structures has thus gained widespread attention. Likewise, there has been a significant focus on designing measures to assess certain topological features of a network by assigning quantitative values to the nodes. **These quantitative values have a subtle interpretation insofar as there are implicit assumptions of the underlying process being carried out on the network.**

of the vertices from most important to least important. The importance of a vertex is relative to the underlying process being carried out on the network. This is why there is a diverse amount of centrality measures addressing many such processes. We propose a measure that assigns a ranking in which interference is a property of the underlying process being carried out on the network.

INTRODUCTION

Networks are perhaps one of the most ubiquitous structures in nature. They can be found in

- cellular biology: connecting genes and proteins,
- neuroscience: connecting regions of the brain,
- sociology: connecting human interactions,
- quantum computing.

Because of networks' ubiquity, the analysis of their underlying topology has gained widespread attention. Likewise, there has been a significant focus on designing measures to assess parts of a network by assigning quantitative values to the nodes. These values can be interpreted many ways because there are implicit assumptions of the processes being carried out on the network.

Borgatti has identified a typology of network flow processes with specific trajectories that use trails, geodesics, paths, or walks. In this framework, the flow has a specific type of transmission corresponding to some concrete application.

Borgatti gives examples such as

- used goods,
- currency,
- infections,
- and gossip.

Our work focused on how to model a flow process in which the flow may interfere with itself. This interference may be the result of collisions in the network, where oppositely-oriented flows may annihilate each other. How can we model such a flow? Our proposition is to model continuous walks on the network until interference occurs.

Anna McEntire 3/16/2015 8:40 PM
Deleted: arise for example

Anna McEntire 3/16/2015 8:40 PM
Deleted: in

Anna McEntire 3/16/2015 8:38 PM
Formatted: List Paragraph, Bulleted + Level: 1 + Aligned at: 0.25" + Indent at: 0.5"

Anna McEntire 3/16/2015 8:40 PM
Deleted: in neuroscience: connectin...

Anna McEntire 3/16/2015 8:40 PM
Deleted: in sociology: connecting th...

Anna McEntire 3/16/2015 8:41 PM
Deleted: and recently in

Anna McEntire 3/16/2015 8:43 PM
Deleted: T...e analysis of their underlyi...

Anna McEntire 3/16/2015 8:45 PM
Comment [1]: DEFINE

Anna McEntire 3/16/2015 8:43 PM
Deleted: quantitative ...alues have a su...

Anna McE..., 3/16/2015 10:11 PM
Formatted: List Paragraph, Bulleted + Level: 1 + Aligned at: 0.25" + Indent at: 0.5"

Anna McE..., 3/16/2015 10:12 PM
Deleted: Suppose we want...to model a ...

Anna McE..., 3/16/2015 10:14 PM
Comment [2]: DEFINE

Anna McE..., 3/16/2015 10:13 PM

Networks are perhaps one of the most ubiquitous structures in nature. They can be found in

- cellular biology: connecting genes and proteins,
- neuroscience: connecting regions of the brain
- sociology: connecting human interactions
- quantum computing.

Because of networks' ubiquity, the analysis of their underlying topology has gained widespread attention. Likewise, there has been a significant focus on designing measures to assess parts of a network by assigning quantitative values to the nodes .

These values can be interpreted many ways because there are implicit assumptions of the processes being carried out on the network.

LEVEL 1:
BE UNDERSTANDABLE



1. DITCH THE JARGON.
2. REDUCE THE CONTENT.

AVERAGE POSTER
VIEW TIME:

2-3

MINUTES

AVERAGE
READING SPEED:

250

WORDS/MINUTE

AVERAGE POSTER
VIEW TIME:

2-3

MINUTES

AVERAGE
READING SPEED:

~~250~~

WORDS/MINUTE

AVERAGE POSTER
VIEW TIME:

2-3

MINUTES

AVERAGE
READING SPEED:

200

WORDS/MINUTE

AVERAGE POSTER
VIEW TIME:

2-3

MINUTES

AVERAGE
READING SPEED:

200

WORDS/MINUTE

WORDS ON POSTER: 600 MAX

AVERAGE POSTER
VIEW TIME:

2-3

MINUTES

AVERAGE
READING SPEED:

200

WORDS/MINUTE

WORDS ON POSTER: ~~600~~ MAX

AVERAGE POSTER
VIEW TIME:

2-3

MINUTES

AVERAGE
READING SPEED:

200

WORDS/MINUTE

WORDS ON POSTER: 400 MAX ?

Investigating mesospheric gravity wave dynamics over McMurdo Station, Antarctica (77° S)

Jonathan R. Pugmire, Mike J. Taylor, Yucheng Zhao, P.-Dominique Pautet
Center for Atmospheric and Space Sciences, Utah State University

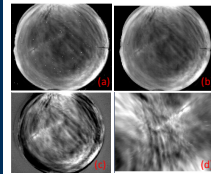
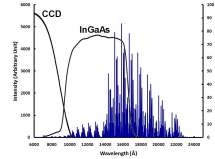
Introduction

The Antarctic Gravity Wave Instrument Network (ANGWIN) is an NSF sponsored international program designed to develop and utilize a network of gravity wave observatories using existing and new instrumentation operated at several established research stations around the continent. Utah State University's Atmospheric Imaging Lab operates all-sky infrared imagers at several research stations. Here we present novel measurements of short-period and larger-scale mesospheric gravity waves imaged during 2012 from McMurdo Station (77.8°S, 166.7°E) on Ross Island. This IR camera has operated at Arrival Heights alongside the University of Colorado Fe Lidar during the past three winter seasons (March-September 2012-2014). Two initial primary goals are:

- Quantify the properties of small- and medium-scale mesospheric gravity wave climatology over this region of Antarctica.
- Combine results with similar measurements from other ANGWIN stations to investigate continental-wide gravity wave dynamics (see SA31B-4100).

IR Imaging

All-sky observations of the OH emission layer (~87 km) were made using an infrared (0.9-1.7 μm) cooled InGaAs camera. The OH airglow emissions are much stronger in the infrared region (>1 μm), as shown in blue in the figure to the right, and we use new InGaAs cameras to obtain high-quality short-exposure images of gravity waves under auroral and full moon observing conditions.



Raw all-sky (180°) OH image data were recorded every 10 s with a 3 s exposure enabling detailed measurements of individual gravity wave events.

- Raw image oriented using the IR star field.
- Stars removed
- Flat fielded: Average nightly image subtracted.
- Unwarped to 350 x 280 km geographic grid at 87 km altitude.

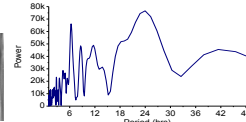
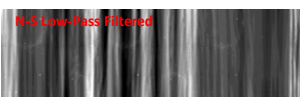
Gravity waves were analyzed using well-developed Fourier analysis techniques to determine direction of propagation (θ), horizontal wavelength (λ), observed horizontal phase speed (v) and wave period (T) [e.g. Taylor, et al, 1997].

During the 2012 observing period (March-September, nighttime hours) at McMurdo over 400 short-period (<1 hr) gravity wave events were observed.



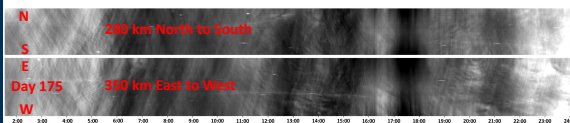
Optical site at Arrival Heights, McMurdo Station

Large-Scale Tidal Analysis



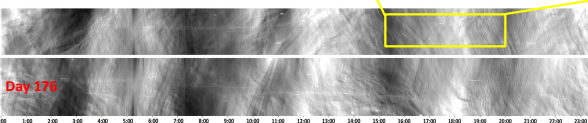
A low-pass filter (>1 hr periods) of the large 73 hour keogram revealing strong tidal features with characteristic periods as identified in the FFT analysis.

FFT power spectrum analysis identifying mesospheric tidal signatures. Note the strong diurnal tide at 24 hours and several harmonics at 6, 8, and 12 hrs.

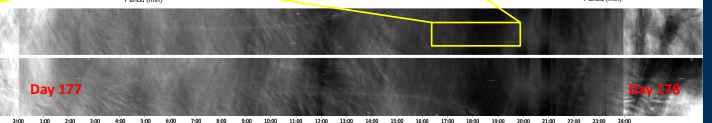


Day 175 200 km North to South

Day 176



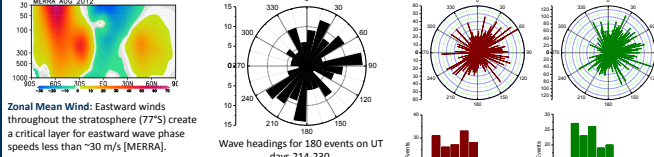
Day 176 350 km East to West



Day 177

Day 178

Two Awesome Weeks in August

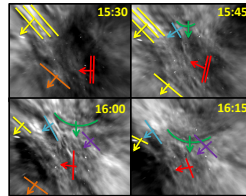


Zonal Mean Wind: Eastward winds throughout the stratosphere (77°S) create a critical layer for eastward wave phase speeds less than ~30 m/s (MERRA).

Wave headings for 180 events on UT days 214-230.

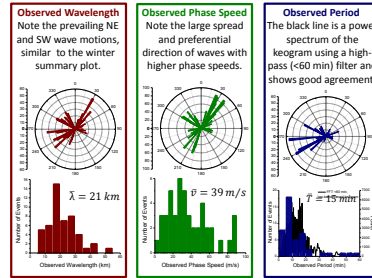
On August 2-18, 2012 (UT day 214-230) over 180 small-scale gravity wave events were observed. Their characteristics were similar to the full season results except their average phase speeds (50 m/s) were significantly higher. These wave events dominated the end of season results. The phase speed distribution is consistent with critical level wind-filtering [Nielson, et al, 2012] with much higher eastward phase speeds.

Three Continuous Days in June



The four unwarped images above show example 350 x 280 km airglow images taken on day 176 every 15 minutes revealing both the high level of wave activity and quality of the images. Several wave features are highlighted as they propagate through the images. The blue and green lines can also be seen in keogram data below, wave event #1.

In mid-winter there is continuous darkness at McMurdo. From June 23-26, 2012 (day 175-178) over 40 small-scale gravity wave events were analyzed during 73 continuous hours of observations. Their properties are shown in the figures below.



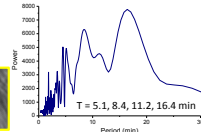
Keograms

Both large- and small-scale gravity wave features can be studied by creating keograms. A keogram is made by stacking vertical (and horizontal) slices through the center of each image together to form a time series revealing wave activity as a function of time. The large keograms along the bottom of the poster shows 73 continuous hours of wave data starting (day 175, 01:33 UT to day 178, 03:09 UT). These data illustrate the high quality of our gravity wave measurements from Antarctica.

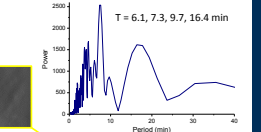
Small-Scale Gravity Waves

A high-pass filter was applied to the keogram to measure small-scale gravity waves with periods of 5-60 min (as highlighted in yellow boxes). Two selected wave events are shown together with their FFT power spectrum. These are compared with the event properties analyzed from the individual airglow images.

Wave Event #1: Day 176, 15:30-19:00
 $\lambda = 22 \pm 3$ km $\theta = 217^\circ \pm 5^\circ$
 $v = 44 \pm 5$ m/s $T = 8 \pm 3$ min

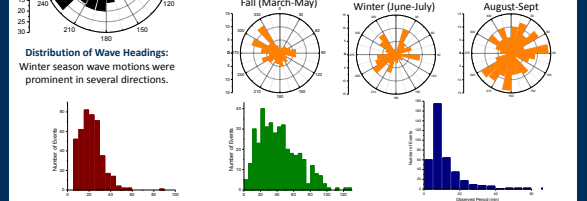


Wave Event #2: Day 177, 16:50-20:00
 $\lambda = 24 \pm 3$ km $\theta = 318^\circ \pm 5^\circ$
 $v = 42 \pm 5$ m/s $T = 10 \pm 3$ min



Summary: 2012 Wave Parameters

The data show evolution from NW propagation (107 events) in the fall which expands to NE and SW wave motions during mid-winter (110 events). The late winter was dominated by many waves (202 events) again exhibiting strong NE and SW motions but more isotropic than earlier. The strong asymmetries are suggestive of localized sources.



Distribution of Wave Headings: Winter season wave motions were prominent in several directions.

Distributions of Observed Wave Parameters

A total of 419 events were analyzed. Their average values were $\lambda = 22$ km, $v = 42$ m/s, $T = 12$ min. These mean values and their ranges are typical for short-period gravity waves observed at several sites around Antarctica as part of ANGWIN.

Summary

We have analyzed one year of data to date from McMurdo Station, Antarctica. The results are as follows:

- A large number (400+) of short-period gravity waves observed over McMurdo, Antarctica enabling the wintertime mesosphere wave climatology to be investigated for the first time.
- McMurdo waves exhibits a large spread of phase speeds with a tendency for high phase speeds up to ~120 m/s.
- New keogram analysis enables the investigation of larger period gravity waves and tidal perturbations in the mesosphere revealing 6, 8, 12, and 24 hr tides and harmonics.
- The sources of the wave events observed from McMurdo are probably associated with strong localized weather systems associated with the polar vortex.
- Small-scale wave event analysis results are comparable using FFT and keograms.



Future Work

- Ongoing measurements from the South Pole station in combination with other ANGWIN sites will be used to investigate pan-Antarctic anisotropy and wave parameters.
- New analysis of McMurdo data from 2013 and 2014 data will further clarify the asymmetries in the wave propagation at this site for understanding the climatology of gravity waves observed at McMurdo.
- Comparison with onsite Fe Boltzmann Lidar measurements and MF radar wind measurements.

References
MERRA Atlas, GEOS-5, August 2012, NASA Goddard Space Flight Center, Retrieved December 11, 2014.
Nielson, K., Taylor, M. J., Hibbins, R. L., Jarvis, M. J., & Russell, J. M. (2012). On the nature of short-period mesospheric gravity wave propagation over Halley, Antarctica. *Journal of Geophysical Research: Atmospheres*, 117(10), 1-10.
Taylor, M.J., W.R. Pendleton, Jr., S. Clark, H. Takahashi, D. Gobbi, and R.A. Goldberg (1997). Image measurements of short-period gravity waves at equatorial latitudes. *J. Geophys. Res.*, 102, 26,283-26,294.
Acknowledgements: This research was supported by NSF grant ANT-1045356.

1,019

WORDS

Investigating mesospheric gravity wave dynamics over McMurdo Station, Antarctica (77° S)

Jonathan R. Pugmire, Mike J. Taylor, Yucheng Zhao, P.-Dominique Pautet
Center for Atmospheric and Space Sciences, Utah State University

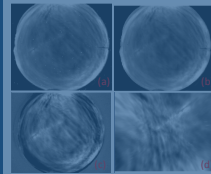
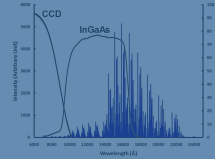
Introduction

The Antarctic Gravity Wave Instrument Network (ANGWIN) is an NSF sponsored international program designed to develop and utilize a network of gravity wave observatories using existing and new instrumentation operated at several established research stations around the continent. Utah State University's Atmospheric Imaging Lidar operates all-sky infrared imagers at several research stations. Here we present novel measurements of short-period and larger-scale mesospheric gravity waves imaged during 2012 from McMurdo Station (77.8°S, 166.7°E) on Ross Island. This IR camera has operated at Arrival Heights alongside the University of Colorado Fe Lidar during the past three winter seasons (March-September 2012-2014). Two initial primary goals are:

- Quantify the properties of small- and medium-scale mesospheric gravity wave climatology over this region of Antarctica.
- Combine results with similar measurements from other ANGWIN stations to investigate continental-wide gravity wave dynamics (see SA31B-4100).

IR Imaging

All-sky observations of the OH emission layer (~87 km) were made using an infrared (0.9-1.7 μm) cooled InGaAs camera. The OH airglow emissions are much stronger in the infrared region (>1 μm), as shown in blue in the figure to the right, and we use new InGaAs cameras to obtain high-quality short-exposure images of gravity waves under auroral and full moon observing conditions.



Raw all-sky (180°) OH image data were recorded every 10 s with a 3 s exposure enabling detailed measurements of individual gravity wave events.

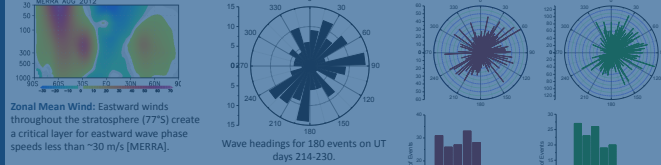
- Raw image oriented using the IR star field.
- Stars removed
- Flat fielded: Average nightly image subtracted.
- Unwarped to 350 x 280 km geographic grid at 87 km altitude.

Gravity waves were analyzed using well-developed Fourier analysis techniques to determine direction of propagation (θ), horizontal wavelength (λ), observed horizontal phase speed (v) and wave period (T) [e.g. Taylor, et al, 1997].

During the 2012 observing period (March-September, nighttime hours) at McMurdo over 400 short-period (<1 hr) gravity wave events were observed.

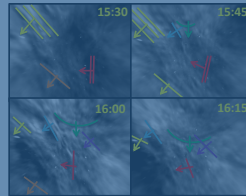


Two Awesome Weeks in August



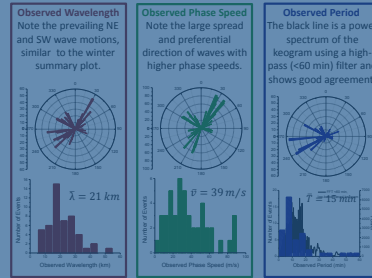
On August 2-18, 2012 (UT day 214-230) over 180 small-scale gravity wave events were observed. Their characteristics were similar to the full season results except their average phase speeds (50 m/s) were significantly higher. These wave events dominated the end of season results. The phase speed distribution is consistent with critical level wind-filtering [Nielson, et al, 2012] with much higher eastward phase speeds.

Three Continuous Days in June



The four unwarped images above show example 350 x 280 km airglow images taken on day 176 every 15 minutes revealing both the high level of wave activity and quality of the images. Several wave features are highlighted as they propagate through the images. The blue and green lines can also be seen in keogram data below, wave event #1.

In mid-winter there is continuous darkness at McMurdo. From June 23-26, 2012 (day 175-178) over 40 small-scale gravity wave events were analyzed during 73 continuous hours of observations. Their properties are shown in the figures below.



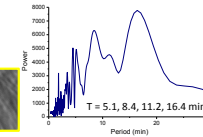
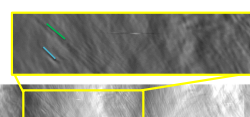
Keograms

Both large- and small-scale gravity wave features can be studied by creating keograms. A keogram is made by stacking vertical (and horizontal) slices through the center of each image together to form a time series revealing wave activity as a function of time. The large keograms along the bottom of the poster shows 73 continuous hours of wave data starting (day 175, 01:33 UT to day 178, 03:09 UT). These data illustrate the high quality of our gravity wave measurements from Antarctica.

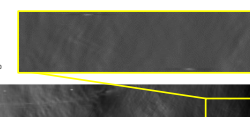
Small-Scale Gravity Waves

A high-pass filter was applied to the keogram to measure small-scale gravity waves with periods of 5-60 min (as highlighted in yellow boxes). Two selected wave events are shown together with their FFT power spectrum. These are compared with the event properties analyzed from the individual airglow images.

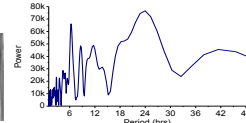
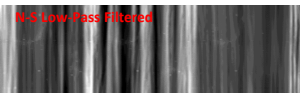
Wave Event #1: Day 176, 15:30-19:00
 $\lambda = 22 \pm 3$ km $\theta = 217^\circ \pm 5^\circ$
 $v = 44 \pm 5$ m/s $T = 8 \pm 3$ min



Wave Event #2: Day 177, 16:50-20:00
 $\lambda = 24 \pm 3$ km $\theta = 318^\circ \pm 5^\circ$
 $v = 42 \pm 5$ m/s $T = 10 \pm 3$ min



Large-Scale Tidal Analysis



FFT power spectrum analysis identifying mesospheric tidal signatures. Note the strong diurnal tide at 24 hours and several identified in the FFT analysis.

N 280 km North to South

S
E
Day 175 380 km East to West

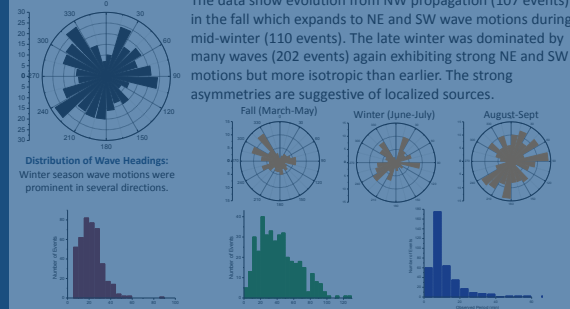
Day 176

Day 177

Day 178

Summary: 2012 Wave Parameters

The data show evolution from NW propagation (107 events) in the fall which expands to NE and SW wave motions during mid-winter (110 events). The late winter was dominated by many waves (202 events) again exhibiting strong NE and SW motions but more isotropic than earlier. The strong asymmetries are suggestive of localized sources.



A total of 419 events were analyzed. Their average values were $\lambda = 22$ km, $v = 42$ m/s, $T = 12$ min. These mean values and their ranges are typical for short-period gravity waves observed at several sites around Antarctica as part of ANGWIN.

Summary

- We have analyzed one year of data to date from McMurdo Station, Antarctica. The results are as follows:
- A large number (400+) of short-period gravity waves observed over McMurdo, Antarctica enabling the wintertime mesosphere wave climatology to be investigated for the first time.
 - McMurdo waves exhibits a large spread of phase speeds with a tendency for high phase speeds up to ~120 m/s.
 - New keogram analysis enables the investigation of larger period gravity waves and tidal perturbations in the mesosphere revealing 6, 8, 12, and 24 hr tides and harmonics.
 - The sources of the wave events observed from McMurdo are probably associated with strong localized weather systems associated with the polar vortex.
 - Small-scale wave event analysis results are comparable using FFT and keograms.



Future Work

- Ongoing measurements from the South Pole station in combination with other ANGWIN sites will be used to investigate pan-Antarctic anisotropy and wave parameters.
- New analysis of McMurdo data from 2013 and 2014 data will further clarify the asymmetries in the wave propagation at this site for understanding the climatology of gravity waves observed at McMurdo.
- Comparison with onsite Fe Boltzmann Lidar measurements and MF radar wind measurements.

References
 MERRA Atlas, GEOS-5, August 2012, NASA Goddard Space Flight Center, Retrieved December 11, 2014.
 Nielson, K., Taylor, M. J., Hibbins, R. L., Jarvis, M. J., & Russell, I. M. (2012). On the nature of short-period mesospheric gravity wave propagation over Halley, Antarctica. *Journal of Geophysical Research: Atmospheres*, 117(10), 10703.
 Taylor, M. J., W. R. Penfold, Jr., S. Clark, H. Takahashi, D. Gobbi, and R. A. Goldberg (1997). Image measurements of short-period gravity waves at equatorial latitudes. *J. Geophys. Res.*, 102, 26,283-26,294.
 Acknowledgements: This research was supported by NSF grant ANT-1045356.

Investigating mesospheric gravity wave dynamics over McMurdo Station, Antarctica (77° S)

Jonathan R. Pugmire, Mike J. Taylor, Yucheng Zhao, P.-Dominique Pautet
Center for Atmospheric and Space Sciences, Utah State University

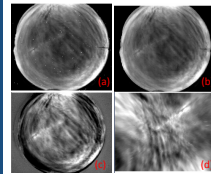
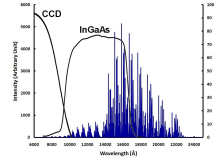
Introduction

The Antarctic Gravity Wave Instrument Network (ANGWIN) is an NSF sponsored international program designed to develop and utilize a network of gravity wave observatories using existing and new instrumentation operated at several established research stations around the continent. Utah State University's Atmospheric Imaging Lab operates all-sky infrared imagers at several research stations. Here we present novel measurements of short-period and larger-scale mesospheric gravity waves imaged during 2012 from McMurdo Station (77.8°S, 166.7°E) on Ross Island. This IR camera has operated at Arrival Heights alongside the University of Colorado Fe Lidar during the past three winter seasons (March-September 2012-2014). Two initial primary goals are:

- Quantify the properties of small- and medium-scale mesospheric gravity wave climatology over this region of Antarctica.
- Combine results with similar measurements from other ANGWIN stations to investigate continental-wide gravity wave dynamics (see SA31B-4100).

IR Imaging

All-sky observations of the OH emission layer (~87 km) were made using an infrared (0.9-1.7 μm) cooled InGaAs camera. The OH airglow emissions are much stronger in the infrared region (>1 μm), as shown in blue in the figure to the right, and we use new InGaAs cameras to obtain high-quality short-exposure images of gravity waves under auroral and full moon observing conditions.



Raw all-sky (180°) OH image data were recorded every 10 s with a 3 s exposure enabling detailed measurements of individual gravity wave events.

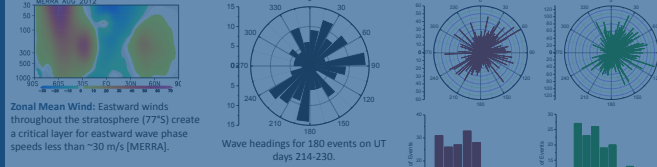
- Raw image oriented using the IR star field.
- Stars removed
- Flat fielded: Average nightly image subtracted.
- Unwarped to 350 x 280 km geographic grid at 87 km altitude.

Gravity waves were analyzed using well-developed Fourier analysis techniques to determine direction of propagation (θ), horizontal wavelength (λ), observed horizontal phase speed (v) and wave period (T) [e.g. Taylor, et al, 1997].

During the 2012 observing period (March-September, nighttime hours) at McMurdo over 400 short-period (<1 hr) gravity wave events were observed.

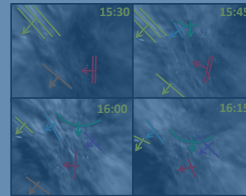


Two Awesome Weeks in August



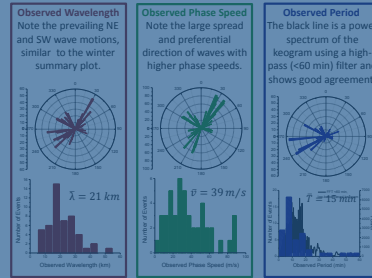
On August 2-18, 2012 (UT day 214-230) over 180 small-scale gravity wave events were observed. Their characteristics were similar to the full season results except their average phase speeds (50 m/s) were significantly higher. These wave events dominated the end of season results. The phase speed distribution is consistent with critical level wind-filtering [Nielson, et al, 2012] with much higher eastward phase speeds.

Three Continuous Days in June



The four unwarped images above show example 350 x 280 km airglow images taken on day 176 every 15 minutes revealing both the high level of wave activity and quality of the images. Several wave features are highlighted as they propagate through the images. The blue and green lines can also be seen in keogram data below, wave event #1.

In mid-winter there is continuous darkness at McMurdo. From June 23-26, 2012 (day 175-178) over 40 small-scale gravity wave events were analyzed during 73 continuous hours of observations. Their properties are shown in the figures below.



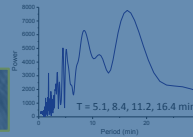
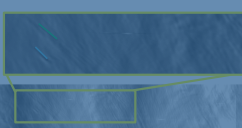
Keograms

Both large- and small-scale gravity wave features can be studied by creating keograms. A keogram is made by stacking vertical (and horizontal) slices through the center of each image together to form a time series revealing wave activity as a function of time. The large keograms along the bottom of the poster shows 73 continuous hours of wave data starting (day 175, 01:33 UT to day 178, 03:09 UT). These data illustrate the high quality of our gravity wave measurements from Antarctica.

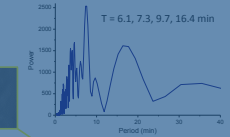
Small-Scale Gravity Waves

A high-pass filter was applied to the keogram to measure small-scale gravity waves with periods of 5-60 min (as highlighted in yellow boxes). Two selected wave events are shown together with their FFT power spectrum. These are compared with the event properties analyzed from the individual airglow images.

Wave Event #1: Day 176, 15:30-19:00
 $\lambda = 22 \pm 3$ km $\theta = 217^\circ \pm 5^\circ$
 $v = 44 \pm 5$ m/s $T = 8 \pm 3$ min

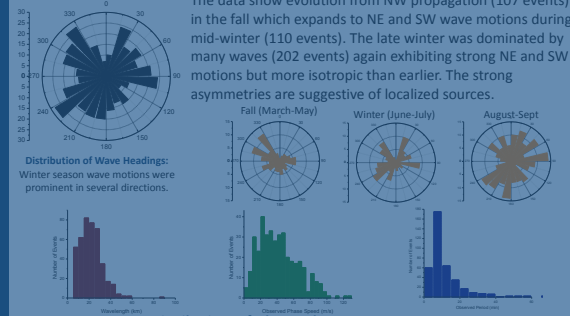


Wave Event #2: Day 177, 16:50-20:00
 $\lambda = 24 \pm 3$ km $\theta = 318^\circ \pm 5^\circ$
 $v = 42 \pm 5$ m/s $T = 10 \pm 3$ min



Summary: 2012 Wave Parameters

The data show evolution from NW propagation (107 events) in the fall which expands to NE and SW wave motions during mid-winter (110 events). The late winter was dominated by many waves (202 events) again exhibiting strong NE and SW motions but more isotropic than earlier. The strong asymmetries are suggestive of localized sources.



A total of 419 events were analyzed. Their average values were $\lambda = 22$ km, $v = 42$ m/s, $T = 12$ min. These mean values and their ranges are typical for short-period gravity waves observed at several sites around Antarctica as part of ANGWIN.

Summary

- We have analyzed one year of data to date from McMurdo Station, Antarctica. The results are as follows:
- A large number (400+) of short-period gravity waves observed over McMurdo, Antarctica enabling the wintertime mesosphere wave climatology to be investigated for the first time.
 - McMurdo waves exhibits a large spread of phase speeds with a tendency for high phase speeds up to ~120 m/s.
 - New keogram analysis enables the investigation of larger period gravity waves and tidal perturbations in the mesosphere revealing 6, 8, 12, and 24 hr tides and harmonics.
 - The sources of the wave events observed from McMurdo are probably associated with strong localized weather systems associated with the polar vortex.
 - Small-scale wave event analysis results are comparable using FFT and keograms.

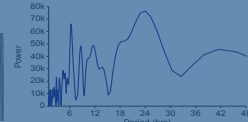
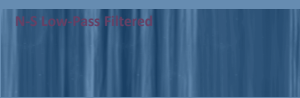


Future Work

- Ongoing measurements from the South Pole station in combination with other ANGWIN sites will be used to investigate pan-Antarctic anisotropy and wave parameters.
- New analysis of McMurdo data from 2013 and 2014 data will further clarify the asymmetries in the wave propagation at this site for understanding the climatology of gravity waves observed at McMurdo.
- Comparison with onsite Fe Boltzmann Lidar measurements and MF radar wind measurements.

References
MERRA Atlas, GEOS-5, August 2012, NASA Goddard Space Flight Center, Retrieved December 11, 2014.
Nielson, K., Taylor, M. J., Hibbins, R. L., Jarvis, M. J., & Russell, I. M. (2012). On the nature of short-period mesospheric gravity wave propagation over Halley, Antarctica. *Journal of Geophysical Research: Atmospheres*, 117(10).
Taylor, M.J., W.R. Pendleton, Jr, S. Clark, H. Takahashi, D. Gobbi, and R.A. Goldberg (1997). Image measurements of short-period gravity waves at equatorial latitudes. *J. Geophys. Res.*, 102, 26,283-26,294.
Acknowledgements: This research was supported by NSF grant ANT-1045356.

Large-Scale Tidal Analysis



A low-pass filter (>1 hr periods) of the large 73 hour keogram revealing strong tidal features with characteristic periods as identified in the FFT analysis.

FFT power spectrum analysis identifying mesospheric tidal signatures. Note the strong diurnal tide at 24 hours and several harmonics at 6, 8, and 12 hrs.

N
S
E
Day 175 350 km East to West
W

Day 176

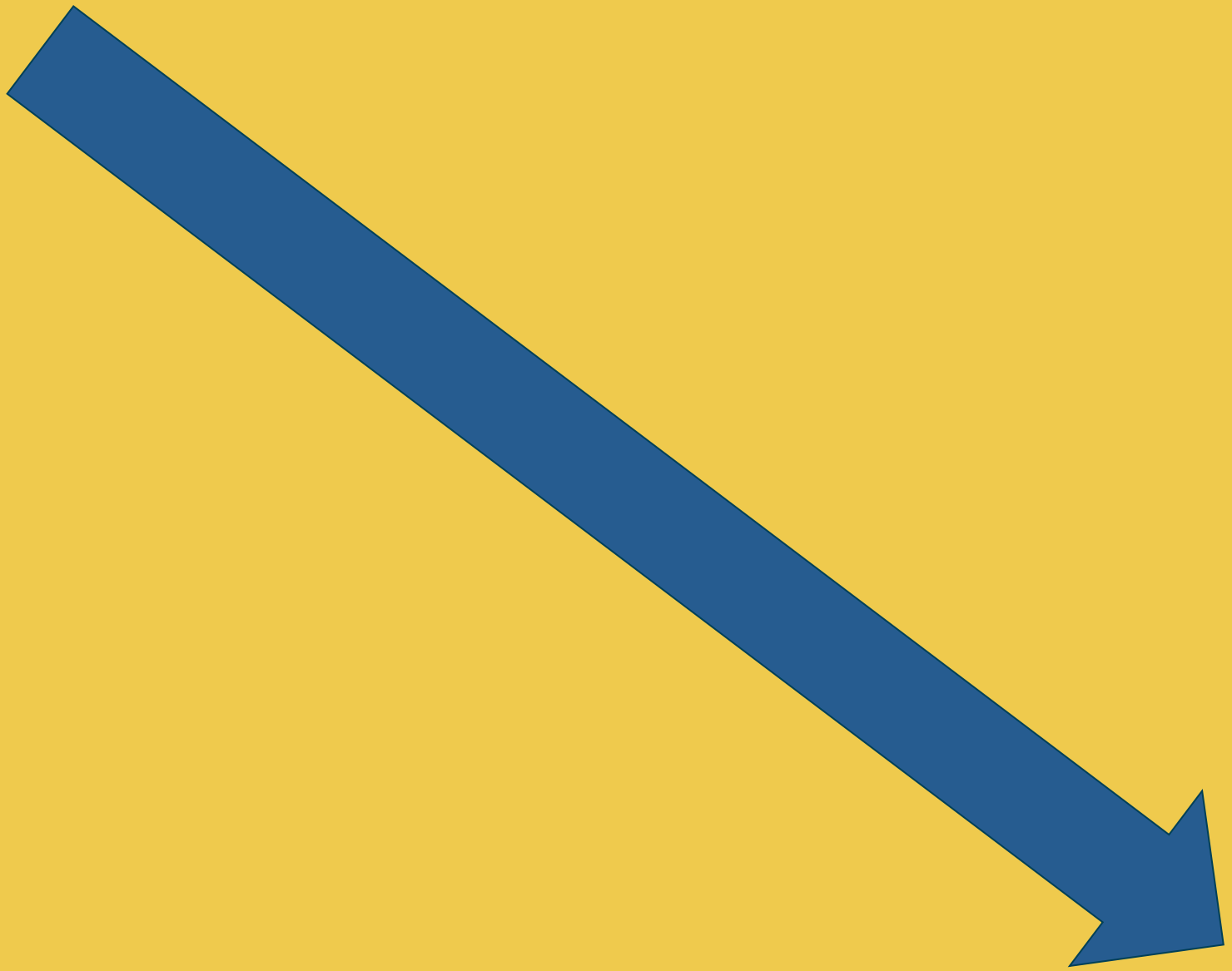
Day 177

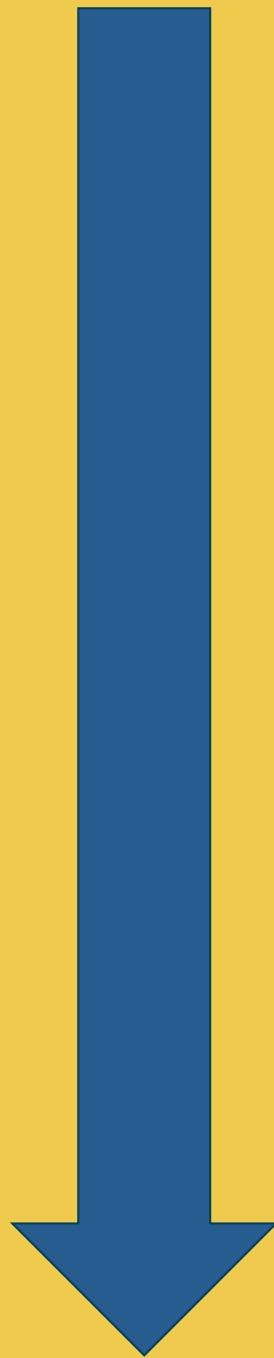
Day 178

LEVEL 1:
BE UNDERSTANDABLE



1. DITCH THE JARGON.
2. REDUCE THE CONTENT.
3. ORGANIZE WHAT'S LEFT.







BUT,











Investigating mesospheric gravity wave dynamics over McMurdo Station, Antarctica (77° S)

Jonathan R. Pugmire, Mike J. Taylor, Yucheng Zhao, P.-Dominique Pautet
Center for Atmospheric and Space Sciences, Utah State University

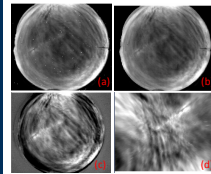
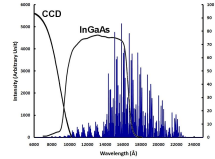
Introduction

The Antarctic Gravity Wave Instrument Network (ANGWIN) is an NSF sponsored international program designed to develop and utilize a network of gravity wave observatories using existing and new instrumentation operated at several established research stations around the continent. Utah State University's Atmospheric Imaging Lab operates all-sky infrared imagers at several research stations. Here we present novel measurements of short-period and larger-scale mesospheric gravity waves imaged during 2012 from McMurdo Station (77.8°S, 166.7°E) on Ross Island. This IR camera has operated at Arrival Heights alongside the University of Colorado Fe Lidar during the past three winter seasons (March-September 2012-2014). Two initial primary goals are:

- Quantify the properties of small- and medium-scale mesospheric gravity wave climatology over this region of Antarctica.
- Combine results with similar measurements from other ANGWIN stations to investigate continental-wide gravity wave dynamics (see SA31B-4100).

IR Imaging

All-sky observations of the OH emission layer (~87 km) were made using an infrared (0.9-1.7 μm) cooled InGaAs camera. The OH airglow emissions are much stronger in the infrared region (>1 μm), as shown in blue in the figure to the right, and we use new InGaAs cameras to obtain high-quality short-exposure images of gravity waves under auroral and full moon observing conditions.



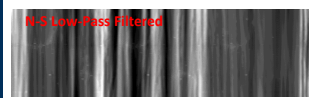
Raw all-sky (180°) OH image data were recorded every 10 s with a 3 s exposure enabling detailed measurements of individual gravity wave events.

- Raw image oriented using the IR star field.
- Stars removed
- Flat fielded: Average nightly image subtracted.
- Unwarped to 350 x 280 km geographic grid at 87 km altitude.

Gravity waves were analyzed using well-developed Fourier analysis techniques to determine direction of propagation (θ), horizontal wavelength (λ), observed horizontal phase speed (v) and wave period (T) [e.g. Taylor, et al, 1997].

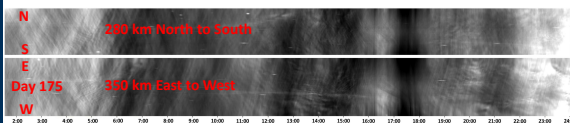
During the 2012 observing period (March-September, nighttime hours) at McMurdo over 400 short-period (<1 hr) gravity wave events were observed.

Large-Scale Tidal Analysis

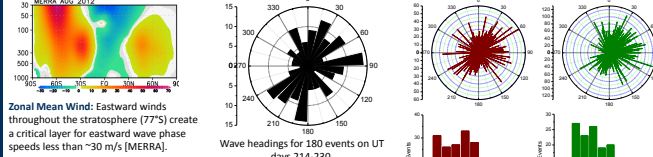


A low-pass filter (>1 hr periods) of the large 73 hour keogram revealing strong tidal features with characteristic periods as identified in the FFT analysis.

FFT power spectrum analysis identifying mesospheric tidal signatures. Note the strong diurnal tide at 24 hours and several harmonics at 6, 8, and 12 hrs.

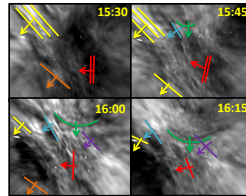


Two Awesome Weeks in August



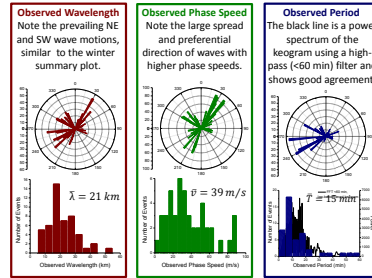
On August 2-18, 2012 (UT day 214-230) over 180 small-scale gravity wave events were observed. Their characteristics were similar to the full season results except their average phase speeds (50 m/s) were significantly higher. These wave events dominated the end of season results. The phase speed distribution is consistent with critical level wind-filtering [Nielson, et al, 2012] with much higher eastward phase speeds.

Three Continuous Days in June



The four unwarped images above show example 350 x 280 km airglow images taken on day 176 every 15 minutes revealing both the high level of wave activity and quality of the images. Several wave features are highlighted as they propagate through the images. The blue and green lines can also be seen in keogram data below, wave event #1.

In mid-winter there is continuous darkness at McMurdo. From June 23-26, 2012 (day 175-178) over 40 small-scale gravity wave events were analyzed during 73 continuous hours of observations. Their properties are shown in the figures below.



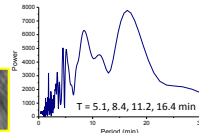
Keograms

Both large- and small-scale gravity wave features can be studied by creating keograms. A keogram is made by stacking vertical (and horizontal) slices through the center of each image together to form a time series revealing wave activity as a function of time. The large keograms along the bottom of the poster shows 73 continuous hours of wave data starting (day 175, 01:33 UT to day 178, 03:09 UT). These data illustrate the high quality of our gravity wave measurements from Antarctica.

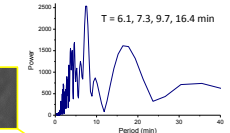
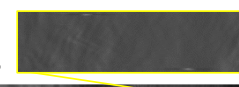
Small-Scale Gravity Waves

A high-pass filter was applied to the keogram to measure small-scale gravity waves with periods of 5-60 min (as highlighted in yellow boxes). Two selected wave events are shown together with their FFT power spectrum. These are compared with the event properties analyzed from the individual airglow images.

Wave Event #1: Day 176, 15:30-19:00
 $\lambda = 22 \pm 3$ km $\theta = 217^\circ \pm 5^\circ$
 $v = 44 \pm 5$ m/s $T = 8 \pm 3$ min

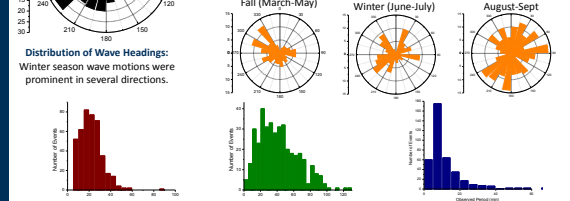


Wave Event #2: Day 177, 16:50-20:00
 $\lambda = 24 \pm 3$ km $\theta = 318^\circ \pm 5^\circ$
 $v = 42 \pm 5$ m/s $T = 10 \pm 3$ min



Summary: 2012 Wave Parameters

The data show evolution from NW propagation (107 events) in the fall which expands to NE and SW wave motions during mid-winter (110 events). The late winter was dominated by many waves (202 events) again exhibiting strong NE and SW motions but more isotropic than earlier. The strong asymmetries are suggestive of localized sources.



A total of 419 events were analyzed. Their average values were $\lambda = 22$ km, $v = 42$ m/s, $T = 12$ min. These mean values and their ranges are typical for short-period gravity waves observed at several sites around Antarctica as part of ANGWIN.

Summary

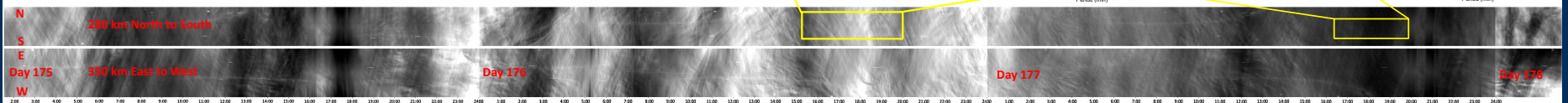
- We have analyzed one year of data to date from McMurdo Station, Antarctica. The results are as follows:
- A large number (400+) of short-period gravity waves observed over McMurdo, Antarctica enabling the wintertime mesosphere wave climatology to be investigated for the first time.
 - McMurdo waves exhibits a large spread of phase speeds with a tendency for high phase speeds up to ~120 m/s.
 - New keogram analysis enables the investigation of larger period gravity waves and tidal perturbations in the mesosphere revealing 6, 8, 12, and 24 hr tides and harmonics.
 - The sources of the wave events observed from McMurdo are probably associated with strong localized weather systems associated with the polar vortex.
 - Small-scale wave event analysis results are comparable using FFT and keograms.



Future Work

- Ongoing measurements from the South Pole station in combination with other ANGWIN sites will be used to investigate pan-Antarctic anisotropy and wave parameters.
- New analysis of McMurdo data from 2013 and 2014 data will further clarify the asymmetries in the wave propagation at this site for understanding the climatology of gravity waves observed at McMurdo.
- Comparison with onsite Fe Boltzmann Lidar measurements and MF radar wind measurements.

References
MERRA Atlas, GEOS-5, August 2012, NASA Goddard Space Flight Center, Retrieved December 11, 2014.
Nielson, K., Taylor, M. J., Hibbins, R. L., Jarvis, M. J., & Russell, J. M. (2012). On the nature of short-period mesospheric gravity wave propagation over Halley, Antarctica. *Journal of Geophysical Research: Atmospheres*, 117(2012), A17705.
Taylor, M.J., W.R. Pendleton, Jr., S. Clark, H. Takahashi, D. Gobbi, and R.A. Goldberg (1997). Image measurements of short-period gravity waves at equatorial latitudes. *J. Geophys. Res.*, 102, 26,283-26,294.
Acknowledgements: This research was supported by NSF grant ANT-1045356.



Investigating mesospheric gravity wave dynamics over McMurdo Station, Antarctica (77° S)

Jonathan R. Pugmire, Mike J. Taylor, Yucheng Zhao, P.-Dominique Pautet
Center for Atmospheric and Space Sciences, Utah State University

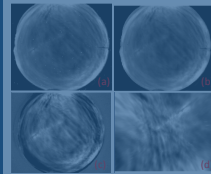
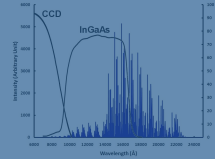
Introduction

The Antarctic Gravity Wave Instrument Network (ANGWIN) is an NSF sponsored international program designed to develop and utilize a network of gravity wave observatories using existing and new instrumentation operated at several established research stations around the continent. Utah State University's Atmospheric Imaging Lidar operates all-sky infrared imagers at several research stations. Here we present novel measurements of short-period and larger-scale mesospheric gravity waves imaged during 2012 from McMurdo Station (77.8°S, 166.7°E) on Ross Island. This IR camera has operated at Arrival Heights alongside the University of Colorado Fe Lidar during the past three winter seasons (March-September 2012-2014). Two initial primary goals are:

- Quantify the properties of small- and medium-scale mesospheric gravity wave climatology over this region of Antarctica.
- Combine results with similar measurements from other ANGWIN stations to investigate continental-wide gravity wave dynamics (see SA31B-4100).

IR Imaging

All-sky observations of the OH emission layer (~87 km) were made using an infrared (0.9-1.7 μm) cooled InGaAs camera. The OH airglow emissions are much stronger in the infrared region (>1 μm), as shown in blue in the figure to the right, and we use new InGaAs cameras to obtain high-quality short-exposure images of gravity waves under auroral and full moon observing conditions.



Raw all-sky (180°) OH image data were recorded every 10 s with a 3 s exposure enabling detailed measurements of individual gravity wave events.

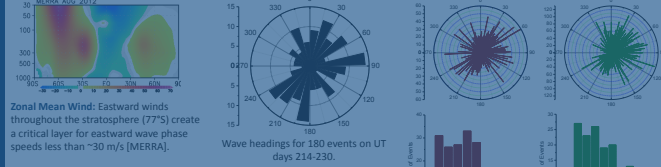
- Raw image oriented using the IR star field.
- Stars removed
- Flat fielded: Average nightly image subtracted.
- Unwarped to 350 x 280 km geographic grid at 87 km altitude.

Gravity waves were analyzed using well-developed Fourier analysis techniques to determine direction of propagation (θ), horizontal wavelength (λ), observed horizontal phase speed (v) and wave period (T) [e.g. Taylor, et al, 1997].

During the 2012 observing period (March-September, nighttime hours) at McMurdo over 400 short-period (<1 hr) gravity wave events were observed.

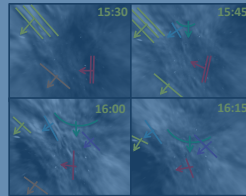


Two Awesome Weeks in August



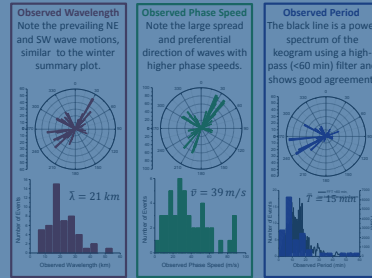
On August 2-18, 2012 (UT day 214-230) over 180 small-scale gravity wave events were observed. Their characteristics were similar to the full season results except their average phase speeds (50 m/s) were significantly higher. These wave events dominated the end of season results. The phase speed distribution is consistent with critical level wind-filtering [Nielson, et al, 2012] with much higher eastward phase speeds.

Three Continuous Days in June



The four unwarped images above show example 350 x 280 km airglow images taken on day 176 every 15 minutes revealing both the high level of wave activity and quality of the images. Several wave features are highlighted as they propagate through the images. The blue and green lines can also be seen in keogram data below, wave event #1.

In mid-winter there is continuous darkness at McMurdo. From June 23-26, 2012 (day 175-178) over 40 small-scale gravity wave events were analyzed during 73 continuous hours of observations. Their properties are shown in the figures below.



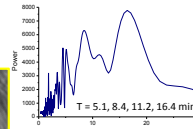
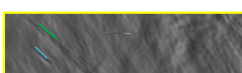
Keograms

Both large- and small-scale gravity wave features can be studied by creating keograms. A keogram is made by stacking vertical (and horizontal) slices through the center of each image together to form a time series revealing wave activity as a function of time. The large keograms along the bottom of the poster shows 73 continuous hours of wave data starting (day 175, 01:33 UT to day 178, 03:09 UT). These data illustrate the high quality of our gravity wave measurements from Antarctica.

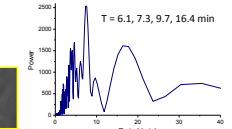
Small-Scale Gravity Waves

A high-pass filter was applied to the keogram to measure small-scale gravity waves with periods of 5-60 min (as highlighted in yellow boxes). Two selected wave events are shown together with their FFT power spectrum. These are compared with the event properties analyzed from the individual airglow images.

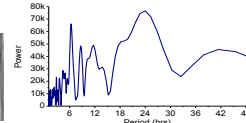
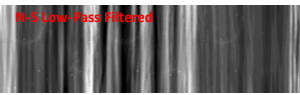
Wave Event #1: Day 176, 15:30-19:00
 $\lambda = 22 \pm 3$ km $\theta = 217^\circ \pm 5^\circ$
 $v = 44 \pm 5$ m/s $T = 8 \pm 3$ min



Wave Event #2: Day 177, 16:50-20:00
 $\lambda = 24 \pm 3$ km $\theta = 318^\circ \pm 5^\circ$
 $v = 42 \pm 5$ m/s $T = 10 \pm 3$ min



Large-Scale Tidal Analysis



FFT power spectrum analysis identifying mesospheric tidal signatures. Note the strong diurnal tide at 24 hours and several identified in the FFT analysis.

N 280 km North to South

S
E
Day 175 380 km East to West

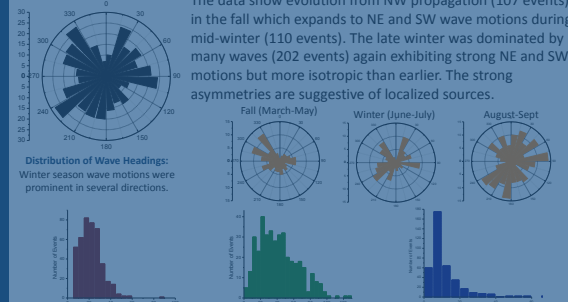
Day 176

Day 177

Day 178

Summary: 2012 Wave Parameters

The data show evolution from NW propagation (107 events) in the fall which expands to NE and SW wave motions during mid-winter (110 events). The late winter was dominated by many waves (202 events) again exhibiting strong NE and SW motions but more isotropic than earlier. The strong asymmetries are suggestive of localized sources.



A total of 419 events were analyzed. Their average values were $\lambda = 22$ km, $v = 42$ m/s, $T = 12$ min. These mean values and their ranges are typical for short-period gravity waves observed at several sites around Antarctica as part of ANGWIN.

Summary

- We have analyzed one year of data to date from McMurdo Station, Antarctica. The results are as follows:
- A large number (400+) of short-period gravity waves observed over McMurdo, Antarctica enabling the wintertime mesosphere wave climatology to be investigated for the first time.
 - McMurdo waves exhibits a large spread of phase speeds with a tendency for high phase speeds up to ~120 m/s.
 - New keogram analysis enables the investigation of larger period gravity waves and tidal perturbations in the mesosphere revealing 6, 8, 12, and 24 hr tides and harmonics.
 - The sources of the wave events observed from McMurdo are probably associated with strong localized weather systems associated with the polar vortex.
 - Small-scale wave event analysis results are comparable using FFT and keograms.



Future Work

- Ongoing measurements from the South Pole station in combination with other ANGWIN sites will be used to investigate pan-Antarctic anisotropy and wave parameters.
- New analysis of McMurdo data from 2013 and 2014 data will further clarify the asymmetries in the wave propagation at this site for understanding the climatology of gravity waves observed at McMurdo.
- Comparison with onsite Fe Boltzmann Lidar measurements and MF radar wind measurements.

References
 MERRA Atlas, GEOS-5, August 2012, NASA Goddard Space Flight Center, Retrieved December 11, 2014.
 Nielson, K., Taylor, M. J., Hibbins, R. L., Jarvis, M. J., & Russell, I. M. (2012). On the nature of short-period mesospheric gravity wave propagation over Halley, Antarctica. *Journal of Geophysical Research: Atmospheres*, 117(16), 17003.
 Taylor, M. J., W. R. Penfold, Jr., S. Clark, H. Takahashi, D. Gobbi, and R. A. Goldberg (1997). Image measurements of short-period gravity waves at equatorial latitudes. *J. Geophys. Res.*, 102, 26,283-26,294.
 Acknowledgements: This research was supported by NSF grant ANT-1045356.

LEVEL 1:
BE UNDERSTANDABLE



1. DITCH THE JARGON.
2. REDUCE THE CONTENT.
3. ORGANIZE WHAT'S LEFT.